TUNABLE DIODE LASER ABSORPTION SPECTROSCOPY OF HYPERSONIC FLOWS

Brad Wheatley
Post-graduate Student, Centre for Hypersonics,
School of Mathematics and Physics, The University of Queensland
b.wheatley@uq.edu.au

Keywords: *laser absorption spectroscopy, hypersonic, scramjet*

Abstract

Re-entrant and scramjet flows involve hypersonic speeds, highly reactive species, ionisation and large heat transfer between the flow and the walls of the body in the flow. Knowing the parameters and species of the flow is important as they drive the reaction rates, heat transfer and forces on the body. For a scramjet, rapidly measuring the species and flow parameters assists in controlling the propellant feed into the combustor.

Tunable diode laser absorption spectroscopy (TDLAS) may be used to provide quantitative data on the density, temperature, pressure, velocity and species concentrations in hypersonic and scramjet flows. These systems measure the absorption of modulated continuous wave laser light. They are of low power, are compact and can measure absorption at multiple wavelengths.

This paper discusses the preliminary work performed in developing a modular TDLAS system that can characterise the species concentrations in hypersonic and scramjet flows.

1 Introduction

Optical imaging of hypersonic flows provides qualitative information on the fluid flow and can provide quantitative data on density, temperature, pressure, velocity and species concentration.[1] Laser-based interferometry and laser-induced fluorescent imaging have been developed over the years to the stage where they are now standard for imaging hypersonic flows. Both of these techniques use high-power pulsed lasers such as Nd:YAG, ruby or dye lasers.

For a scramjet, rapidly measuring the species and flow parameters assists in controlling the propellant fed into the combustor.[2] Re-entrant flows involve hypersonic speeds, highly reactive species, ionisation and heat transfer between the flow and the body of the vehicle as illustrated in Figure 1. Radiation contributes over 80% of incident heat flux at speeds over 8.5 km s^{-1}.[3] The Thermal Protection Systems (TPS) of re-entry vehicles are designed with large margins of safety to account for uncertainties in the flow parameters and species concentrations with consequent uncertainty in the radiant heat load on the vehicle.[4]

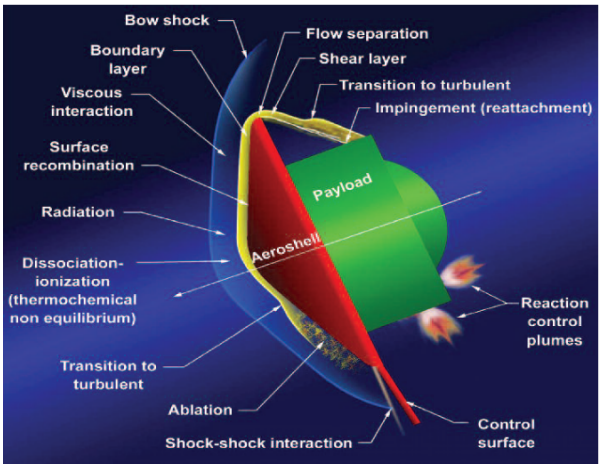

Fig. 1 Physical processes acting on a hypersonic re-entry vehicle [5]

A tunable diode laser absorption spectroscopy (TDLAS) system can also assist an observer to calibrate computational fluid dynamics models and detect changes in species concentrations in hypersonic and scramjet flows at the microsecond scale.[6] This knowledge may improve the design of scramjets and re-entry vehicles.

The author is currently developing a modular TDLAS system to measure species concentrations and parameters in hypersonic and scramjet flows within the test facilities at The University of Queensland. This paper provides a summary of the progress to date.

2 Development of TDLAS Systems

The first TDLAS system was developed in 1978 when Canadian researchers used a lead-salt diode to measure atmospheric gas concentrations for pollution studies.[7] The diode was cooled using cryogenic helium to a temperature in the range of 10 K to 70 K.

Absorption techniques were not initially used in laser spectrometry due to a lack of intensity stabilised sources and fluctuations in the transmission of the optical systems.[8] The development of single-mode diode lasers led to the development of TDLAS systems that used wavelength modulation absorption spectrometry to measure absorption. Diode lasers are of low power, are compact and can be used to measure absorption at multiple wavelengths simultaneously. These characteristics have enabled researchers to simultaneously measure multiple characteristics of the flow such as temperature, pressure, velocity and species concentrations.

The introduction of room temperature tunable laser diodes allowed researchers to expand into making measurements of hypersonic flows in blow-down and shock tunnels. In the early 1990s, Stanford researchers began to apply TDLAS to combustion and scramjet studies. In 1992, Arroyo and Hanson [9] developed a TDLAS system to measure water vapour concentration and temperature at room temperature and in a methane-air flame at 1720 K.

Since the turn of the century, researchers in the United States have continued developing TDLAS systems for scramjet combustion monitoring.[6, 10, 11] In Australia, Griffiths [12] constructed a system for time-resolved temperature and water vapour concentration measurements in a scramjet combustor. Their system probed two absorption lines near 1390 nm at rates up to 20 kHz using two time-multiplexed lasers.

The system being developed by the author is based on that of Griffiths but is also modular and can detect multiple chemical species simultaneously.

3 Theory

A TDLAS system relies on the absorption of radiation by gaseous molecules or atoms to determine the temperature, pressure and species concentration in the flow. Kluczynski [8] provides an extensive review of the signal generation process for wavelength modulation absorption spectrometry. Cai et al [13] designed and developed a TDLAS system that monitored combustion in a flame by measuring the gas temperature and the H_2O concentration. The system used a single near-infrared diode laser based on the second-harmonic detection of the wavelength modulation spectroscopy (WMS-2f). Cai's analysis is used as the basis for this presentation of TDLAS theory.

3.1 Fundamental Relationships

The transmission coefficient $\tau(\nu)$ of monochromatic laser radiation through a uniform gas is given by the Beer-Lambert relation:

$$\begin{aligned} \tau(\nu) &= \left(\frac{I_t}{I_0}\right)_\nu \\ &= \exp\left[-\alpha(\nu)\right] \end{aligned}$$

where I_0 is the incident laser intensity, I_t is the intensity of the transmitted radiation and $\alpha(\nu)$ is the spectral absorbance of the sample. An optically thin sample has a spectral absorbance $\alpha(\nu) < 0.1$ so the exponential term may be ap-

proximated by a first order Taylor-series expansion:

$$\tau(\nu) \approx 1 - \alpha(\nu)$$

If the incident laser radiation is modulated to a modulation depth a (cm^{-1}) at an angular frequency $\omega = 2\pi f$, the instantaneous frequency of the radiation at time t (s) is given by:

$$\nu(t) = \overline{\nu} + a\cos(\omega t)$$

where $\overline{\nu}$ is the centre frequency for the laser. The equation for the instantaneous frequency may be substituted into the equation for spectral absorbance giving:

$$\alpha(\nu) = \alpha[\overline{\nu} + a\cos(\omega t)]$$

For a gaseous sample of total pressure P (atm) and path length l (cm) with a mole fraction x of the absorbing species and a line strength S_j (cm^{-2} atm^{-1}) of the transition of absorption feature j, the spectral absorbance may be re-written as:

$$\alpha(\nu) = Pxl\sum_j S_j(T)\phi_j(\nu)$$

Here, the line strength $S_j(T)$ is a function of the gas temperature T (K) and $\phi_j(\nu)$ (cm) is the line shape function for the feature. The line shape function is normalised such that:

$$\int \phi(\nu)\, d\nu = 1$$

Thus, spectral absorbance is an even periodic function in ωt that may be expanded in a Fourier cosine series:

$$\alpha[\overline{\nu} + a\cos(\omega t)] = -\sum_{n=0}^{\infty} H_k(\overline{\nu}, a)\cos(n\omega t)$$

where the components $H_k(\overline{\nu}, a)$ are given by:

$$\begin{aligned} k = 0: \\ H_0(\overline{\nu}, a) &= -\frac{Pxl}{2\pi}\int_{-\pi}^{\pi}\sum_j S_j\phi_j(\overline{\nu} + a\cos\theta)\, d\theta \\ k > 0: \\ H_k(\overline{\nu}, a) &= -\frac{Pxl}{\pi}\int_{-\pi}^{\pi}\sum_j S_j\phi_j(\overline{\nu} + a\cos\theta)\cos(k\theta)\, d\theta \end{aligned}$$

These components have a number of features that are important to TDLAS applications. Firstly, if the line shape function does not vary for the conditions of the test, H_k is directly proportional to species concentration and path length. Secondly, H_k depends on the modulation depth of the incident laser radiation. The modulation index m is defined as:

$$m = \frac{a}{\Delta\nu_{\frac{1}{2}}}$$

where $\Delta\nu_{\frac{1}{2}}$ is the half-width at half maximum (HWHM) of the absorption line shape. Note that this is not the HWHM of the laser radiation but is a function of the gas and test properties.

3.2 Detecting Intensity changes

Two features of laser diodes are that the output power and wavelength emitted depend on the diode temperature and current. Within limits, selecting an appropriate temperature/current combination provides an output power at a selected wavelength. Space limitations restrict the discussion of laser diodes here. Interested readers are encouraged to refer to texts such as [14, 15] for further information.

One of three methodologies is usually employed to detect the intensity changes in TDLAS systems: direct detection, first harmonic ($1f$) detection and second harmonic ($2f$) detection. The earliest systems detected the direct absorption across the sample (that is, $\alpha(\nu)$). This is equivalent to having H_0 as the only component of the spectral absorbance function. These measurements were susceptible to laser power variations, noise and other losses [7] so first harmonic detection was introduced.

For first harmonic detection, the laser diode current is modulated using a saw-tooth, sinusoidal or other cyclical method. The instantaneous incident intensity $I_0(t)$ is then:

$$I_0(t) = \bar{I}_0[1 + i_o\cos(\omega t + \psi_1)]$$

This introduces a linear modulation component to the laser intensity of amplitude i_0. The receiver measures changes in the linear

$i_o \cos(\omega t + \psi_1)$ term with a phase shift ψ_1 due to the sample absorbance. With $1f$ detection, the noise level was dramatically reduced but the received signal still varied with laser injection current.[7]

Second harmonic detection uses two modulation components to the laser intensity: a linear modulation of intensity amplitude i_0 and phase shift ψ_1, and a non-linear modulation of intensity amplitude i_2 and phase shift ψ_2, where i_1 and i_2 are normalised by the average intensity of the incident laser radiation ($\bar{I}_0$). The instantaneous incident intensity $I_0(t)$ in this case is:

$$I_0(t) = \bar{I}_0 [1 + i_o \cos(\omega t + \psi_1) + i_2 \cos(2\omega t + \psi_2)]$$

Second harmonic $(2f)$ detection measures changes in the non-linear $i_2 \cos(2\omega t + \psi_2)$ term. The $2f$ signal is detected by multiplying the signal by a sinusoidal reference signal at frequency 2ω. The magnitude of the $2f$ signal is given by:[13]

$$S_{2f}(\overline{\nu}) = \frac{G\bar{I}_o}{2} \left| H_2 - \frac{i_0}{2}(H_1 + H_3) \right|$$

where G is the optical-electrical gain of the detection system.

Second harmonic detection has emerged as the method that has the least noise and gives the best detection sensitivities. Cai et al [13] used a small modulation depth ($a = 0.053$ cm^{-1}) which meant that $i_2 \approx 0$ near the line centre of the discrete spectra. Thus, the contribution of the non-linear term was neglected. The magnitude of the $2f$ signal near the line centre becomes:

$$S_{2f}(\overline{\nu}) = \frac{GI_o H_2}{2}$$

Also, the linear term phase shift ψ_1 was assumed to be equal to π. The magnitude of the $1f$ signal near the line centre is:

$$S_{1f}(\overline{\nu}) = \frac{G\bar{I}_o}{2} \left| H_1 - i_0 \left(H_0 + \frac{H_2}{2} \right) \right|$$

Near the line centre, H_0 is unity, H_2 is a maximum and H_1 and H_3 are zero. Therefore, near the line centre the dominant term in the $2f$ signal is the H_2 term whilst the dominant term in the $1f$ signal is H_0. The $2f$ signal, normalised by the $1f$ signal is:

$$C = \frac{S_{2f}}{S_{1f}} = \frac{|H_2 - i_0(H_1 + H_3)/2|}{|H_1 - i_0(H_0 + H_2)/2|}$$

The spectral line shape may be a Gaussian function (if Doppler broadening dominates), a Lorentzian function (if pressure broadening dominates) or a Voigt function between these two extremes.[16] Most often, TDLAS systems assume that the Voigt function applies and use an algorithm due to Humlicek [17] to evaluate the function. May et al [16] provides guidance on processing harmonic detection data that is output by TDLAS systems.

This theoretical derivation is complicated practically by uncertainties in the gas temperature, absorption by species other than the target, chemical reactions in the flow, atmospheric absorption and other sources of noise in the detection electronics.

4 Wavelength Selection

A target species must be in sufficient concentration and must absorb or emit radiation at a suitable wavelength to be a candidate for TDLAS monitoring. Each target species has numerous absorption or emission peaks depending on the reactions taking place and on the flow temperature and pressure. The wavelength selected for a TDLAS also depends on the availability of laser diodes, photodetectors and optics. Choosing a strong absorption peak may be irrelevant if there are no commercially available laser diodes or photodetectors at that wavelength. This is particularly relevant for detecting water vapour as many of the cheapest and most readily available laser diodes have been developed for electronics or telecommunications. These diodes tend to avoid wavelengths where water vapour absorbs strongly. This section discusses wavelength selection for three potential applications of TDLAS: Earth atmospheric entry, Martian atmo-

spheric entry and scramjet combustor measurements.

As an example of the atmospheric entry conditions for an Earth re-entry, Figure 2 shows a spectrum generated from a test in the X2 tunnel using air as the test gas. The conditions for this experiment simulate those experienced by a space vehicle entering the atmosphere at high speed.[18] This spectrum shows strong features for atomic O and N as well as singly ionised N. The Al, C and S features are most likely due to contaminants whilst the Hα feature may be due to dissociated water vapour. Based on this type of data, the author has selected the 844.6 nm oxygen feature for investigation by TDLAS. The 777 nm features were not selected because suitable optical components at a reasonable price were not available.

For a TDLAS system applied to atmospheric entry to Mars, Titan or Jupiter, the atmospheric composition for that body needs to be considered. For example, the chemical composition of the Martian atmosphere is 95-96% CO_2, 2.7% N_2, 0.6% Ar, 0.13% O_2, 0.07% CO, 0.03% H_2O and 0.013% NO.[19] During a Mars entry, the velocity will be in the range $5.8 - 9$ kms^{-1}.[19] The translational temperatures behind the shock wave (prior to vibrational onset excitation) corresponding to these flight speeds in a Martian atmosphere range from 25 000 K to 59 000 K respectively while the equilibrium temperatures range from 4800 K to 7300 K.[3, 19] Under these conditions, CN is a significant radiator. Ideally, the 388.3 nm CN violet feature would be used for TDLAS due to its strength [20] however, the author was not able to find suitable laser diodes and photodiodes for this wavelength. Instead, the CN feature at 916.8 nm was selected for analysis.[21, 22]

The measurement wavelengths for scramjets were selected based on previous research and on reviews of spectral modelling programs such as HITRAN [23] and HITEMP [24]. HITRAN is an excellent source for atmospheric spectra. HITEMP is analogous to the HITRAN database but encompasses many more bands and transitions than HITRAN for the absorbers H_2O, CO_2, CO, NO, and OH. Whilst the spectral databases have advantages, they also pose a number of potential risks including errors in the reported line strengths especially at high temperature, and missing or additional spectral lines at high temperature.[12] Table 1 provides a summary of the wavelengths that have been previously investigated. Given the number of scramjet TDLAS systems operated in the range 1391-1393 nm, the 1392.53 nm feature was selected for this system.

Wavelength(nm) (nm)	Wavenumber (cm^{-1})	Source
1340.12	7462.00	[25]
1343.30	7444.37	[26]
1343.30	7444.35	[26]
1380.00	7246.38	[9]
1391.67	7185.60	[26]
1391.79	7185.00	[25]
1392.53	7181.16	[12]
1392.81	7179.75	[12]
1405.09	7117.00	[25]
1468.90	6807.83	[26]

Table 1 Previously investigated scramjet water vapour features

The wavelength choice is ultimately a compromise between the best theoretical choice and one where optical components are commercially available. After deciding on the species of interest and the wavelength for observation, the flow conditions, flow enthalpy and target species in the test area influence the TDLAS system design and operation. To illustrate this, the X2 expansion tunnel is described below.

5 X2 Expansion Tunnel

The X2 Expansion Tunnel is an impulse facility operated as a dual-driver expansion tunnel as shown in Figure 3. A high pressure air reservoir propels a single-stage piston down the 257 mm diameter driver tube compressing a helium/argon driver gas that ruptures a scored steel primary diaphragm.

An 85 mm bore tube is connected to the driver tube. In expansion tunnel mode this sec-

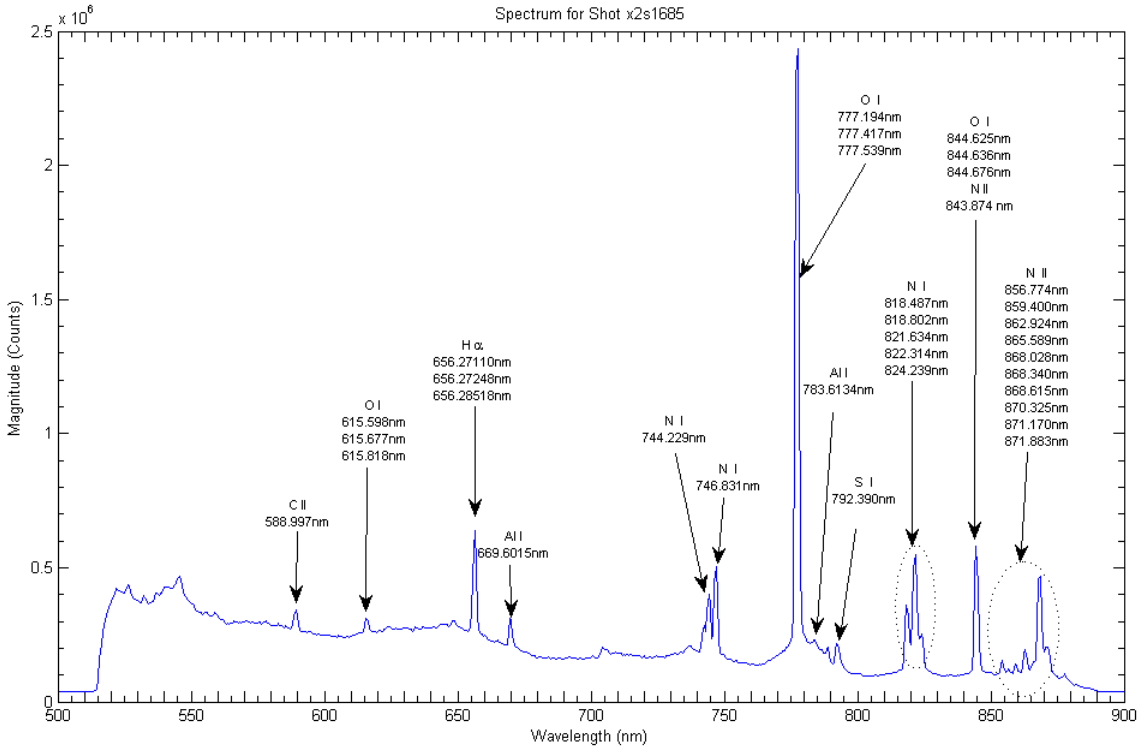

Fig. 2 Typical spectrum for an X2 test using air as a test gas (Test X2s1685)

tion is separated into secondary, tertiary and acceleration tubes by thin mylar or aluminium diaphragms. The tertiary diaphragm initiates an unsteady expansion of the test gas into low pressure air that provides the total enthalpy and pressure multiplication unique to expansion facilities. A Mach 10 full capture hypersonic nozzle with an area ratio of 6 is attached to the end of the acceleration tube, providing a nominal core flow of approximately 100 mm.

Figure 3 includes a so-called X-T diagram that shows how the tunnel components, shock waves and expansion waves change with test time. The time axis starts at primary diaphragm rupture. The compressed driver gas is in region (4). The secondary gas is indicated by (1) and the acceleration gas is indicated by (10). After the primary diaphragm ruptures, a primary shock waves travels down the secondary tube compressing the secondary (or test) gas (1). At the same time, the driver gas undergoes an unsteady expansion (3). The secondary (test) gas is separated from the driver gas as indicated by region (2). The secondary diaphragm ruptures next resulting in a secondary shock and compression of the acceleration gas as shown by region (20). The secondary gas also undergoes un unsteady expansion as it moves down the acceleration tube. The test time is shown by region (5). It is the time after the acceleration gas passes the model and before the test gas expansion wave strikes the model. There are also two reflected shocks as indicated by the $u+a$ waves in the X-T diagram.

High enthalpy flows such as those found in expansion tubes and shock tunnels produce test times in the order of 50 μs to 1 ms.[3] This places extreme demands on a TDLAS system that relies on wavelength modulation. The modulation frequency must be at least 1 MHz. During the test time, the flow and the species behind the shock wave change considerably. Thus, the laser diodes and photodetector circuits must have response rates of the order of nano-seconds. Figure 4 is an image of a test body in an expansion

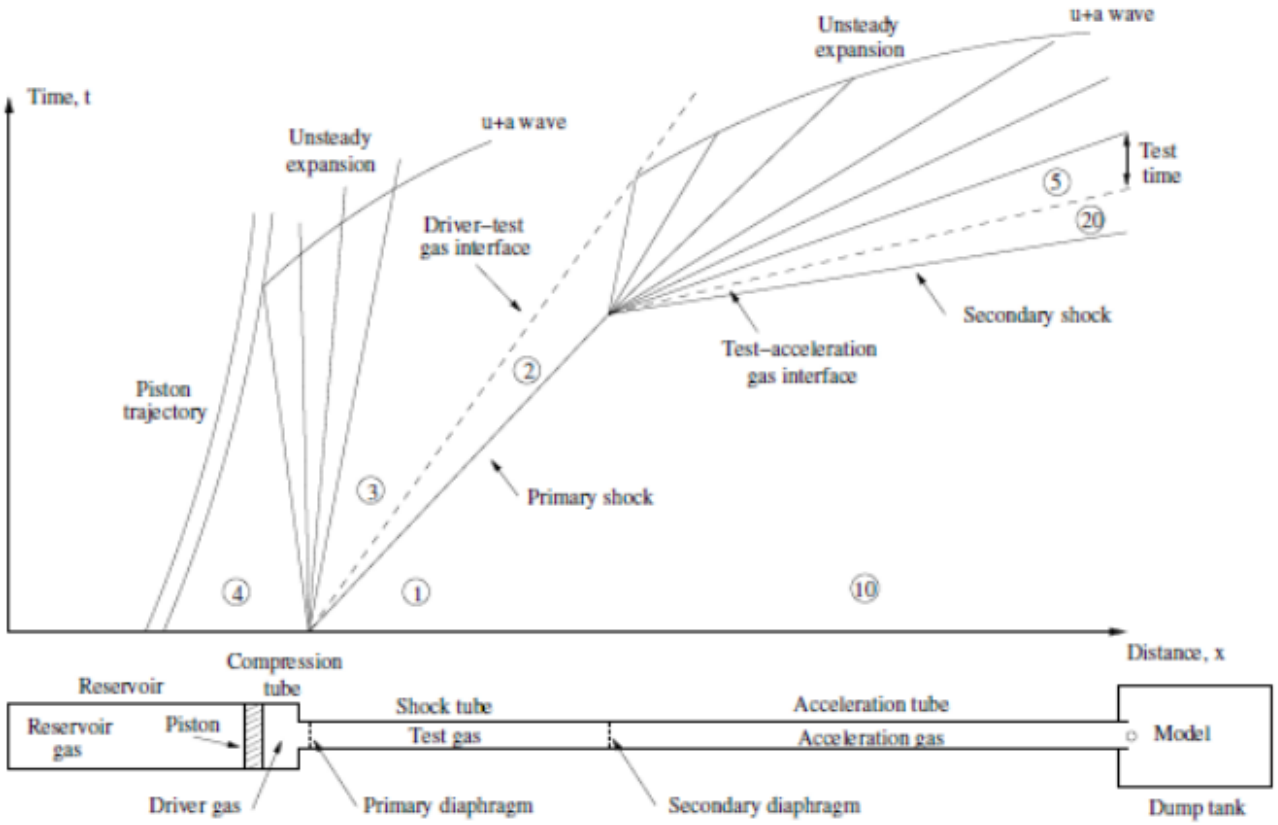

Fig. 3 X-T diagram and schematic of an expansion tunnel [27]

tube. This image was taken with a Shimadzu HPV-1 camera at 1 million frames per second. It provides an indication of the relationship between the test body and the bow shock. Ideally, the TDLAS system should be able to determine the species concentrations in front and behind the bow shock. The test area is approximately 2-4 mm in cross-section.

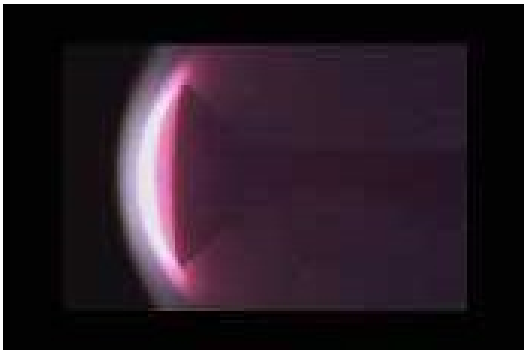

Fig. 4 Image of bow shock in expansion tube test

6 System Design

The TDLAS system has been designed to be modular and adaptable to various test scenarios. Figure 5 is a high-level schematic of the system. It comprises a Transmission sub-system (TSS) (Figure 6), a Receiver sub-system (RSS) (Figure 7) and a Data Recording sub-system (DRSS). The TSS is now discussed in more detail to illustrate the design concept.

6.1 TSS

The TSS consists of a Thorlabs PRO8000 Laser Diode Controller with up to eight Thorlabs ITC-8052 modules, each of which controls a laser diode. Each laser diode is mounted on a thermistor mount (typically Thorlabs TLDM-9) that

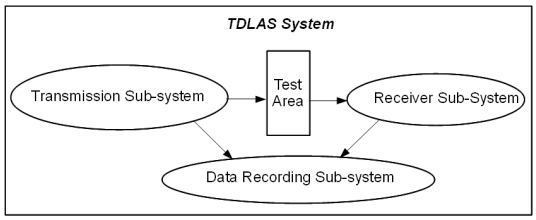

Fig. 5 TDLAS System

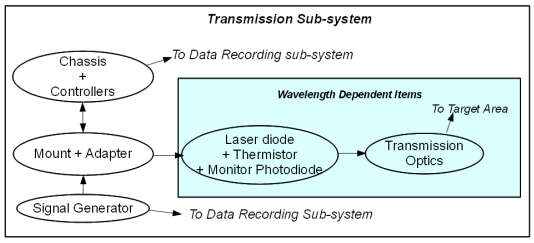

Fig. 6 Transmission Sub-system

controls the diode temperature and current based on signals from the controller. The controller is also connected to a desktop computer via an Ines GPIB-USB-2 cable that allows the user to program the controller prior to a test. The laser diode current schedule as well as up to nine measurement parameters can be preset for one thousand (or less) test points in one test.

Figure 8 is a schematic layout of the Wavelength Dependent Transmission (WDT) group. As many as eight WDT groups can be controlled simultaneously. This group consists of the optical elements of the TSS. The laser diode may be either collimated for free-space transmission or its output may be injected into an optical fibre for transmission directly into the test area. A beamsplitter (typically 8% reflectance-92%transmittance) may be used to measure the power output from the laser diode for correlation

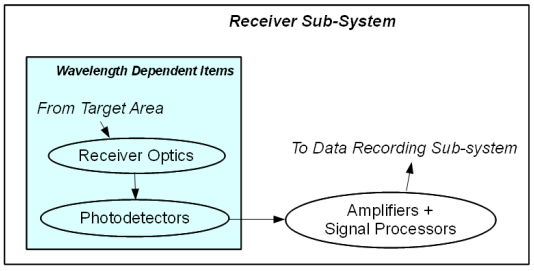

Fig. 7 Receiver Sub-system

with the received signal that has passed through the test area. If water vapour is the target species, the TSS components should be encased in atmospheric isolators that are purged with nitrogen to avoid unwanted absorption.

7 Conclusion

Using a TDLAS system to measure species concentrations in hypersonic and scramjet flows allows an observer to calibrate computational fluid dynamics models, measure flow parameters and detect changes in species concentrations at the microsecond scale. This paper has discussed the theoretical basis for TDLAS systems, highlighted their application to hypersonic and scramjet tests and described the high-level design of a system being developed by the author at The University of Queensland. The system is currently being tested and will be shortly implemented in the facility.

8 Acknowledgments

The author acknowledges the financial support of The University of Queensland and the professional support from the members of the Centre for Hypersonics.

8.1 Copyright Statement

References

[1] McIntyre TJ, Kleine H, and Houwing AFP. Optical imaging techniques for hypersonic impulse

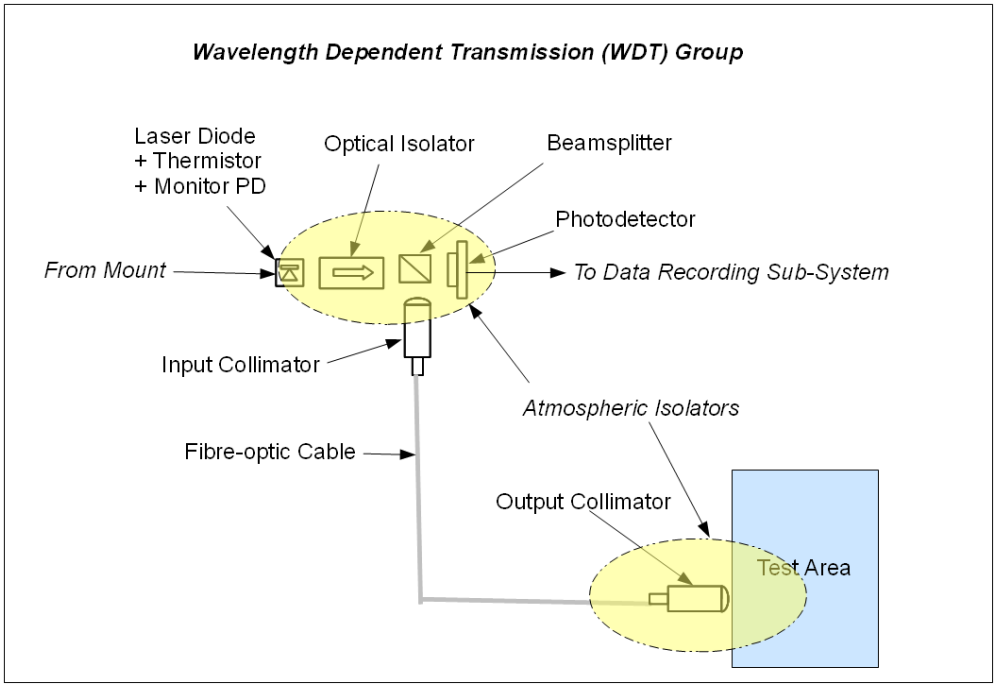

Fig. 8 Wavelength Dependent Transmission Group

facilities. *Aeronautical Journal*, 111(1115):1 – 16, 2007.

[2] Segal C. *Scramjet Engine: Processes and Characteristics*. Cambridge University Press, Cambridge, 2009.

[3] Potter DF, Gollan RJ, Eichmann TB, McIntyre TJ, Morgan RG, and Jacobs PA. Simulation of CO_2-N_2 expansion tunnel flows for the study of radiating shock layers. *46th AIAA Aerospace Sciences Meeting and Exhibit*, 2008.

[4] Capra BR and Morgan RG. Radiative and total heat transfer measurements to a Titan explorer model. *4th AIAA/AHI Space Planes and Hypersonic Systems and Technologies Conference*, 2006.

[5] NASA. Hypersonics research. Internet fact sheet. Downloaded from www.nasa.gov on 24 October 2011.

[6] Lindstrom CD, Jackson KR, Williams S, Givens R, Bailey WF, Tam CJ, and Terry WF. Shock-train structure resolved with absorption spectroscopy. Part 1: System design and validation. *AIAA Journal*, 47(10):2368 – 78, 2009.

[7] Reid J, Shewchun J, Garside BK, and Ballik EA. High sensitivity pollution detection employing tunable diode lasers. *Appl. Opt.*, 17(2):300–307, Jan 1978.

[8] Kluczynski P, Gustafsson J, Lindberg AM, and Axner O. Wavelength modulation absorption spectrometry - An extensive scrutiny of the generation of signals. *Spectrochimica Acta Part B: Atomic Spectroscopy*, 56(8):1277 – 1354, 2001.

[9] M.P. Arroyo and R.K. Hanson. Absorption measurements of water vapor concentration, temperature, and line-shape parameters using a tunable InGaAsP diode laser. *Appl. Opt.*, 32(30):6104–6116, Oct 1993.

[10] Lindstrom CD, Davis D, Williams S, and Tam CJ. Shock-train structure resolved with absorption spectroscopy. Part 2: Analysis and CFD comparison. *AIAA Journal*, 47(10):2379 – 90, 2009.

[11] Brown MS, Williams S, Lindstrom CD, and Barone DL. Progress in applying tunable diode laser absorption spectroscopy to scramjet isolators and combustors. Technical Report AFRL-RZ-WP-TP-2010-2146, Air Force Research Laboratory, United States, May 2010.

[12] Griffiths AD and Houwing AFP. Diode laser absorption spectroscopy of water vapor in a scram-

jet combustor. *Appl. Opt.*, 44(31):6653–6659, Nov 2005.

[13] Cai T, Wang G, Jia H, and Gao X. Temperature and water concentration measurements in combustion gases using a DFB diode laser at 1.4 microns. *Laser Physics*, 18(10):1133, 2008.

[14] Amann M-C. *Tunable Laser Diodes*. Artech House, Norwood, MA USA, 1998.

[15] Sands D. *Diode Lasers*. Institute of Physics Publishing, Bristol UK, 2005.

[16] May RD and Webster CR. Data processing and calibration for tunable diode laser harmonic absorption spectrometers. *Journal of Quantitative Spectroscopy and Radiative Transfer*, 49(4):335 – 347, 1993.

[17] Humlícek J. Optimized computation of the Voigt and complex probability functions. *Journal of Quantitative Spectroscopy and Radiative Transfer*, 27(4):437 – 444, 1982.

[18] Eichmann TB, Khan R, McIntyre TJ, Jacobs CM, Porat H, Buttsworth DR, and Upcroft B. Radiometric temperature analysis of the Hayabusa spacecraft re-entry. In *28th International Symposium on Shock Waves*, Manchester, UK, 2011.

[19] Park C, Howe JT, Jaffe RL, and Candler GV. Review of chemical-kinetic problems of future NASA missions, II: Mars entries. *Journal of Thermophysics and Heat Transfer*, 8(1):9–22, 1994.

[20] Hornkohl JO, Parigger C, and Lewis JWL. Temperature measurements from CN spectra in a laser-induced plasma. *Journal of Quantitative Spectroscopy and Radiative Transfer*, 46(5):405 – 411, 1991.

[21] Parker AE. Analysis of the (0,0) $^2\Pi \rightarrow ^2\Sigma$ CN band at 9168Å. *Phys. Rev.*, 41(3):274–277, Aug 1932.

[22] Cerny D, Bacis R, Guelachvili R, and Roux F. Extensive analysis of the red system of the CN molecule with a high resolution Fourier spectrometer. *Journal of Molecular Spectroscopy*, 73(1):154 – 167, 1978.

[23] Rothman LS, Gordon IE, Barbe A, Benner DC, Bernath PF, Birk M, Boudon V, Brown LR, Campargue A, Champion J-P, Chance K, Coudert LH, Dana V, Devi VM, Fally S, Flaud J-M, Gamache RR, Goldman A, Jacquemart D, Kleiner I, Lacome N, Lafferty WJ, Mandin J-Y, Massie ST, Mikhailenko SN, Miller CE, Moazzen-Ahmadi N, Naumenko OV, Nikitin AV, Orphal J, Perevalov VI, Perrin A, Predoi-Cross A, Rinsl CP, Rotger M, Simecková M, Smith MAH, Sung K, Tashkun SA, Tennyson J, Toth RA, Vandaele AC, and Vander Auwera J. The HITRAN 2008 molecular spectroscopic database. *Journal of Quantitative Spectroscopy and Radiative Transfer*, 110(9-10):533 – 572, 2009.

[24] Rothman LS, Gordon IE, Barber RJ, Dothe H, Gamache RR, Goldman A, Perevalov VI, Tashkun SA, and Tennyson J. HITEMP, the high-temperature molecular spectroscopic database. *Journal of Quantitative Spectroscopy and Radiative Transfer*, 111(15):2139 – 2150, 2010. XVIth Symposium on High Resolution Molecular Spectroscopy (HighRus-2009), XVIth Symposium on High Resolution Molecular Spectroscopy.

[25] Nagali V, Herbon JT, Horning DC, Davidson DF, and Hanson RK. Shock-tube study of high-pressure H_2O spectroscopy. *Appl. Opt.*, 38(33):6942–6950, Nov 1999.

[26] Liu JTC, Rieker GB, Jeffries JB, Gruber MR, Carter CD, Mathur T, and Hanson RK. Near-infrared diode laser absorption diagnostic for temperature and water vapor in a scramjet combustor. *Appl. Opt.*, 44(31):6701–6711, Nov 2005.

[27] Scott MP. *Development and Modelling of Expansion Tubes*. PhD thesis, The University of Queensland, 2006.